Disease Models & Mechanisms 6, 252-260 (2013) doi:10.1242/dmm.009886

Characterising the tumour morphological response to therapeutic intervention: an ex vivo model

Anne Savage[1,*], Elad Katz[2,*,‡], Alistair Eberst[1], Ruth E. Falconer[3], Alasdair Houston[3], David J. Harrison[2,4] and James Bown[1]

SUMMARY

In cancer, morphological assessment of histological tissue samples is a fundamental part of both diagnosis and prognosis. Image analysis offers opportunities to support that assessment through quantitative metrics of morphology. Generally, morphometric analysis is carried out on two-dimensional tissue section data and so only represents a small fraction of any tumour. We present a novel application of three-dimensional (3D) morphometrics for 3D imaging data obtained from tumours grown in a culture model. Minkowski functionals, a set of measures that characterise geometry and topology in *n*-dimensional space, are used to quantify tumour topology in the absence of and in response to therapeutic intervention. These measures are used to stratify the morphological response of tumours to therapeutic intervention. Breast tumours are characterised by estrogen receptor (ER) status, human epidermal growth factor receptor (HER)2 status and tumour grade. Previously, we have shown that ER status is associated with tumour volume in response to tamoxifen treatment ex vivo. Here, HER2 status is found to predict the changes in morphology other than volume as a result of tamoxifen treatment ex vivo. Finally, we show the extent to which Minkowski functionals might be used to predict tumour grade. Minkowski functionals are generalisable to any 3D data set, including in vivo and cellular systems. This quantitative topological analysis can provide a valuable link among biomarkers, drug intervention and tumour morphology that is complementary to existing, non-morphological measures of tumour response to intervention and could ultimately inform patient treatment.

INTRODUCTION

In cancer, the morphological assessment of histological tissue samples is a fundamental part of both diagnosis and prognosis (Beck et al., 2011). Histopathological grading is subjective (Wöhlke et al., 2011) and there exists substantial variability among individual pathologists (Fanshawe et al., 2008). Moreover, particular morphological phenomena such as tumour budding, characterised by relatively small clusters of tumour cells becoming detached from the main tumour body, are known to be indicators of prognosis but are difficult to describe quantifiably and objectively (Wang et al., 2009). Morphometric image analysis has the potential to aid standardisation of interpretation of histopathology samples, extending to the postsurgical development of carcinomas (Eynard et al., 2009). Moreover, advances in laboratory methods provide quantitative, objective data platforms upon which morphometric image analysis can be founded (Wöhlke et al., 2011). Morphometric image analysis can be undertaken at a range of scales including (combinations of) subcellular, cellular and tissue scale (Eynard et al., 2009) and with a diversity of quantitative computational tools (Yaffe, 2008). For example, Beck and co-workers describe a software tool that can integrate an impressive range of quantitative morphometrics of breast cancer epithelium and the stroma (Beck et al., 2011). Their analysis considered a range of data scales: fine-scale analyses include nuclei size and shape; higher level analyses explore sample structure, including relation measures such as mean distance between typical and atypical nuclei in stroma and epithelial tissues. They demonstrated that a set of multiscale features in cancer stroma are significantly associated with survival. Other work has characterised tissue structure itself, including measures of area and texture. Given the link between risk of development of breast cancer and breast tissue density (Boehm et al., 2008), area measures of different tissue densities are of prognostic value in some but not all case studies (Yaffe, 2008).

Textural measures characterise the morphological features of tissue, in particular the distribution of parenchymal and stromal tissue (Boehm et al., 2008). A common approach is to characterise tissue by its fractal dimension, which provides a measure of self-similarity and, thus, irregularity in an object (Franzén et al., 2008). Fractal geometry has been applied to a range of different cancers and in conjunction with other measures (Goutzanis et al., 2009). For example, it was explored whether the fractal dimension of nuclear chromatin might be used as a predictor of survival in melanoma patients (Bedin et al., 2010). The invasive front of colon carcinomas was quantified in terms of a complexity index based on fractal dimension complemented by the number of tumour cell clusters (Franzén et al., 2008). This complexity index was tested against independent pathology classification and performed better than fractal dimension alone.

Another metric set used in texture analysis is Minkowski functionals, a family of statistical metrics able to characterise *n*-dimensional space geometrically and topologically (Arns et al., 2010). Two-dimensional (2D) images can be described by three Minkowski functionals: area fraction, boundary length and the

[1]Centre for Research in Informatics and Systems Pathology (CRISP), University of Abertay Dundee, Dundee, DD1 1HG, UK
[2]Division of Pathology, University of Edinburgh, Edinburgh, EH4 2XU, UK
[3]SIMBIOS, University of Abertay Dundee, Dundee, DD1 1HG, UK
[4]School of Medicine, University of St Andrews, KY16 9SS, UK
*These authors contributed equally to this work
‡Author for correspondence (elad.katz@ed.ac.uk)

Received 21 March 2012; Accepted 8 August 2012

TRANSLATIONAL IMPACT

Clinical issue

Carcinomas make up at least 80% of human solid tumours. As the cancer progresses, the transformed epithelia spread locally into the connective tissue (stroma), ultimately forming local and distal metastases. The spread of cancer thus occurs in three-dimensional (3D) space. This has been modelled in vitro using extracellular matrix-based tissue culture models. In breast research, compliant collagen type I or basement-membrane extract have been used successfully to model both normal development and cell transformation. Nevertheless, the analysis of 3D cultures is almost exclusively undertaken using only 2D techniques, which are frequently based on microscopic analysis of formalin-fixed sample sections. Thus, there is a lack of knowledge regarding the 3D morphological properties of human cancer as it occurs naturally and of 3D culture-based cancer models. Quantitative morphometrics of cancer spread would allow direct comparisons of tumour grade and biomarkers. Furthermore, they would enable measurements of drug responses in a 3D context.

Results

This paper shows that Minkowski functionals – a set of statistical metrics that characterise geometry and topology in *n*-dimensional space – can be used to quantify tumour topology in the absence of and in response to therapeutic intervention. The authors applied these measures to investigate human breast cancer ex vivo spread. First, they report that Minkowski functionals are closely correlated with clinically determined tumour grade. Second, they find that estrogen-negative (ER–) breast tumours exposed to tamoxifen ex vivo undergo morphological changes that cannot be observed using volumetric measurements alone. Third, HER2 status in estrogen-positive (ER+) tumours seems to predict their responsiveness to tamoxifen as determined by Minkowski functionals.

Implications and future directions

Tumours are a 3D entity, and their direct and indirect effects, including invasion and metastasis, depend on their 3D characteristics. This paper presents a quantitative method for analysing cancer spread and response to therapy in 3D models. This method is broadly applicable to the study of various cancer types and established 3D tumour models. Being able to quantify aspects of 3D growth, and to measure the effects of therapy and environment, opens up new avenues for biomarker exploration.

Euler number (Mattfeldt et al., 2007), and these have been used to characterise tissue samples and have been linked to pathology classification using 2D images of breast tissue. Minkowski functionals were used for images segmented into phases of stroma, epithelium and luminal space. In this instance, data area fraction of the epithelium phase was a strong indicator of the presence of a mammary carcinoma. Minkowski functionals have also been used to classify 2D X-ray attenuation patterns of breast tissue (Boehm et al., 2008). Against independent clinical classification, Minkowski functionals were able to classify tissue into three categories (fibrotic, atrophic and normal) far better than chance.

Most morphological studies, including those noted above, consider 2D tissue sections. Volume measures in three dimensions (3D) are likely to be of even greater prognostic value (Yaffe, 2008). A recent study has linked morphometric data from 3D culture-based tumours to gene expression data (Han et al., 2010). Morphometric analysis was undertaken on a large number of 2D images of those tumours, and this morphological profile was linked to gene expression data in two ways: first, clusters of morphologically similar cell lines were determined and genes that discriminated among clusters identified; and, second, genes that were able to discriminate among separate morphological features were identified. The first analysis determined broad associations between phenotype and genotype and the second analysis linked particular features of specific cell lines to gene expression, suggesting mechanisms linking phenotype and genotype.

We reported previously on a 3D culture model, which enables the spread of human breast cancer ex vivo, within stromal type I collagen. Volumetric analysis of breast cancers in this system showed that response to drugs such as tamoxifen mimics responses seen in the clinic (Leeper et al., 2012). Specifically, we observed a significant effect of tamoxifen treatment on tumour volume for estrogen receptor-positive (ER+), but not estrogen receptor-negative (ER–) tumours. Here, we describe investigation into the impact of tamoxifen on morphological characteristics other than volume. To do this, we characterised tumours grown in 3D cultures using Minkowski functionals. We show how these topological characteristics might be used to stratify morphological response of tumours to therapeutic intervention in a complementary manner to the existing range of tumour-response biomarkers. We make the novel observation that human epidermal growth factor receptor (HER)2 status can predict the changes in morphology resulting from tamoxifen treatment ex vivo. Finally, we show the extent to which Minkowski functionals can be used to predict tumour grade.

RESULTS

Preliminary analysis

Three-dimensional images can be described by four Minkowski functionals that relate to volume, surface area, integral mean curvature (IMC) and integral total curvature (ITC) (see Materials and Methods for further details). The volume and surface area of the tumour are readily understood. IMC and ITC are measures of curvedness and connectedness, respectively, and both are signed quantities. IMC is a numerical summation of the average curvature at each point on the detected surface of the tumour. A locally convex surface makes a positive contribution and locally concave surfaces make a negative contribution. Smooth surfaces are expected to have lower magnitude IMC values relative to more rugged surfaces. The topological measure ITC describes the connectedness of tumour fragments detected within an image; large values of ITC are indicative of complex tumours such as those with invading fingers.

Fig. 1 shows reconstructed optical projection tomography (OPT) images for three illustrative tumours. Fig. 1A shows a tumour with low IMC and high ITC, with a smooth spheroidal main body and significant protrusions on one side. Fig. 1B shows a tumour with high IMC and high ITC, with a combination of an aspherical tumour body and several protrusions. Fig. 1C shows a tumour with high IMC and low ITC; the tumour is rugged on its surface with no substantial protrusions.

Using Minkowski functionals, we determined associations between tamoxifen treatment status and either ER status or HER2 status for all tumours. In addition to ER and HER2 status of each of the 30 tumour explant preparations and information on whether or not a tumour had been treated by tamoxifen, supplementary material Table S1 provides the results of analysis, with absolute values for all functional measures. Also included are two measurements of tumour aggressiveness: lymph node status and tumour grade.

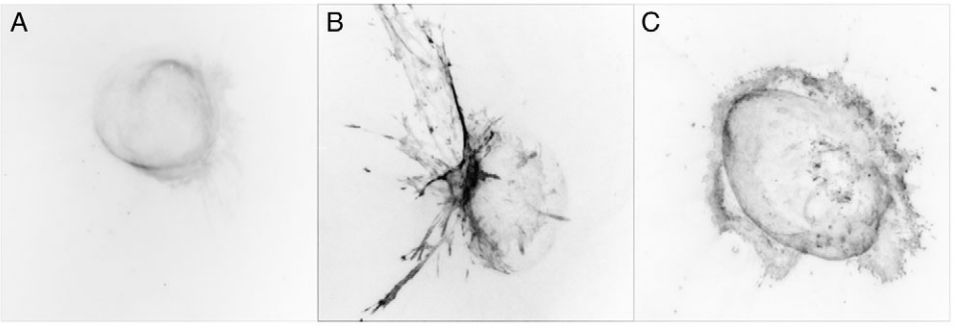

Fig. 1. Illustrative 2D sections of OPT scan source data for three tumours. (A) ER–, HER2– tumour treated with tamoxifen with low (smooth) IMC and high Euler characteristic (protrusions), ITC; (B) Untreated ER+, HER2+ tumour with high IMC (rugged) and high ITC; (C) ER–, HER2+ tumour treated with tamoxifen with a low ITC (no protrusions) and high IMC (rugged). Note that Minkowski functionals are calculated on the basis of segmented image files and normalised by volume. Image contrast in the original OPT scan data has been enhanced for photographic reproduction purposes (but not for analysis).

In order that volume effects did not dominate morphological analysis, we normalised all surface area, IMC and ITC values by volume. For surface area and IMC this provides us with measures of surface area per unit volume (SA/V; density of tumour surface per tumour volume) and curvature per unit volume (IMC/V; density of tumour surface curvature per tumour volume), respectively. Tumours with lower SA/V values are more spherical; tumours with lower IMC/V values are less rugged overall. Moreover, the normalisation of IMC and surface area was supported by the strong correlation between both of these functionals and volume (P<0.01). This correlation is intuitively reasonable in that, for a fixed resolution, larger volume tumours will have a greater surface area and IMC than morphologically similar but smaller tumours. The normalisation was also applied to ITC for reasons of consistency across Minkowski functionals, though not clearly indicated by a significant correlation with volume.

Fig. 2 shows IMC/V, ITC/V and SA/V values for treated and untreated tumours, with both IMC/V and ITC/V plotted against SA/V. Fig. 2A,C depict tumours without tamoxifen treatment; Fig. 2B,D depict tumours with tamoxifen treatment. The effect of tamoxifen on Minkowski functional values is clearly shown. Generally, treated tumours have lower values of SA/V and IMC/V (Fig. 2, compare A with B) and ITC/V (Fig. 2, compare C with D) than untreated tumours and, therefore, tamoxifen application results in tumours that are rounder, smoother and less fingered.

In our plots of Minkowski functionals for tumours with and without treatment we also highlight the tumour subtype: ER and HER2 status tumours in Figs 2 and 3, respectively. Note that the tumours in Fig. 3 are identical in their Minkowski functional values to those in Fig. 2 and so the points overlap. The difference between the two figures lies in the patterning of ER and HER2 status across the treated and untreated tumours. In Fig. 2A-D there is no clear distinction between patterns for ER+ and ER– in either treated or untreated tumour sets. Likewise, Fig. 3A,C (untreated tumours) shows no clear distinction between HER2+ and HER2– status tumours. Notably, we observed a clear separation based on HER2

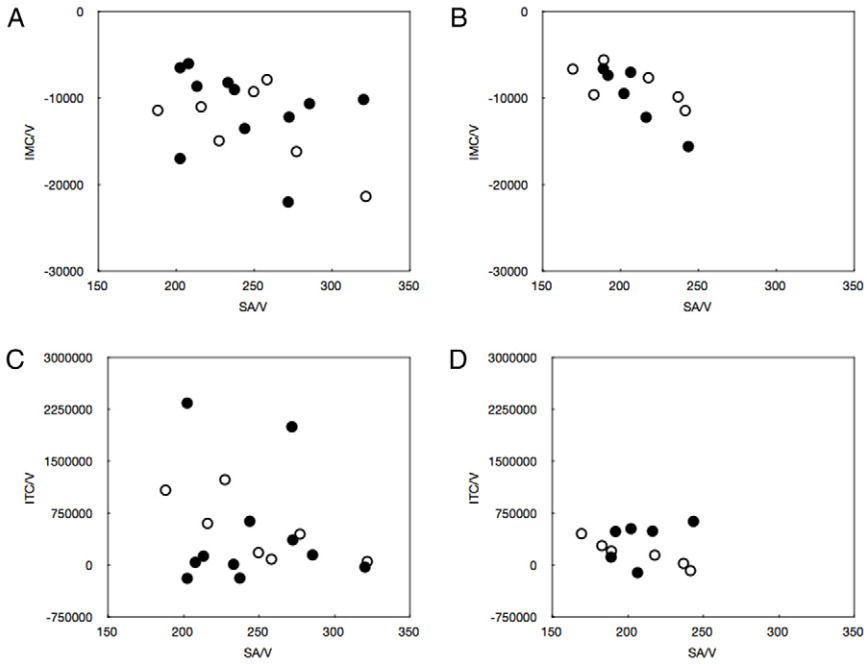

Fig. 2. Plots of Minkowski functionals IMC, ITC and surface area normalised by volume. (A,C) IMC/V and ITC/V, respectively, plotted against SA/V for untreated tumours. (B,D) IMC/V and ITC/V respectively plotted against SA/V for tamoxifen-treated tumours. ER status confers no clear discrimination in morphological response to tamoxifen. Open circles, ER–; closed circles, ER+.

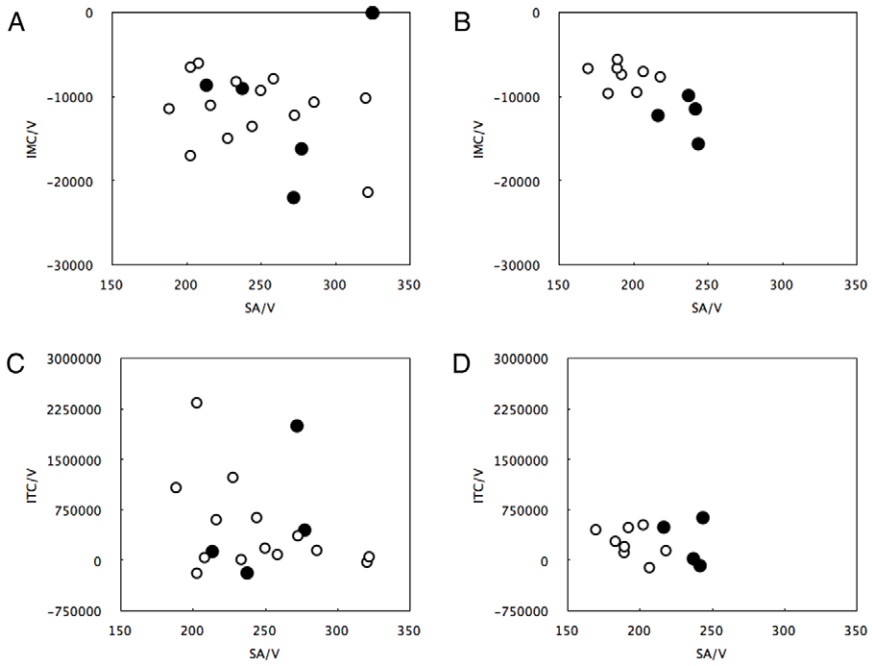

Fig. 3. Plots of Minkowski functionals IMC, ITC and surface area normalised by volume. (A,C) IMC/V and ITC/V, respectively, plotted against SA/V for untreated tumours. (B,D) IMC/V and ITC/V, respectively, plotted against SA/V for tamoxifen-treated tumours. HER2 status offers a clear separation between tumours, especially in B. Open circles, HER2–; closed circles, HER2+.

status for treated tumours (Fig. 3B,D), with HER2– tumours being more responsive in terms of morphological change to tamoxifen treatment than HER2+ tumours for IMC/V and SA/V but not ITC/V.

From this preliminary analysis, we hypothesised that that HER2 status provides better stratification of morphological response to tamoxifen treatment than ER status.

Characterising the influence of tamoxifen and tumour subtype on morphology

We sought to determine the influence of four categorical explanatory variables (tamoxifen treatment, ER status, HER2 status and node status) on the set of quantitative morphological response variables (IMC/V, ITC/V and SA/V). Because we considered the influence of four explanatory variables on three measures of morphology, individual pair-wise comparisons could not take into account other, possibly confounding, variables. An added complication was that we did not have equal numbers of tumours in each category (see supplementary material Table S1). Data of this type can be analysed by factorial analysis of variance by regression, where all explanatory variables are factors. Like multiple linear regression, this analysis makes use of the general linear model where the response variable (IMC/V, ITC/V and SA/V) is modelled and the contributions of each factor and the interactions between factors in the model assessed.

We first considered the effect of tamoxifen treatment, ER status, HER2 status and node status on the morphological descriptors IMC/V, ITC/V and SA/V for all tumours. Table 1 shows the contributions of these explanatory variables on the Minkowski functionals responses. The addition of tamoxifen into the model is significant for SA/V, has a strong but not significant effect (P=0.07) for IMC/V and has no significant effect for ITC/V. The addition of HER2 into the model had a significant effect for IMC/V and SA/V but not for ITC/V. We also observed a significant effect from the introduction of an interaction between ER and node status. The inclusion of all other explanatory variables and interactions had no significant effect on the model.

We next considered the influence of tumour subtype (ER± and HER2± status) on tamoxifen response, together with the effects of HER2 status on ER± tumour response and ER status on HER2± tumour response. For ER-based tumour analysis, we also included node status because of the observed interaction between ER and node status shown in Table 1.

Table 2 shows the contributions of tamoxifen treatment and HER2 status for tumours that are ER+ and for tumours that are ER–. For ER+ tumours, the addition of tamoxifen to the model was significant for SA/V but not for IMC/V or ITC/V. For ER– tumours, the addition of tamoxifen to the model was significant for IMC/V and SA/V but not for ITC/V. The addition of node status into the model was significant for SA/V and ITC/V. All other factors for all response variables were not significant.

We compared treated and untreated tumours for both ER+ and ER– tumours using a t-test assuming unequal sample size and equal variance. Specifically, treated ER+ tumours had a significantly lower SA/V value than untreated tumours [all values expressed as mean ± s.d.; treated SA/V 208.55±19.95, untreated SA/V 244.92±38.70; $t(15)$=2.13, P=0.05]. Treated ER– tumours had a significantly smaller IMC/V value than untreated tumours [treated IMC/V −8,424.49±2,215.07; untreated IMC/V −13,109.15±4,661.70; $t(11)$=2.2, P=0.05]. Note that, for ER– tumours SA/V was lower in treated tumours than in untreated tumours and this was nearly significant (P=0.07). There were no other significant differences in morphological characteristics for ER+ or ER– tumours.

Table 3 shows the contributions of tamoxifen treatment and ER status for tumours that are HER2+ and for tumours that are HER2–. For HER2+ tumours, there were no significant factors for any response variable. For HER2– tumours, the addition of tamoxifen to the model was significant for IMC/V and SA/V but not for ITC/V, and all other factors for all response variables were not significant. When comparing treated and untreated HER2– tumours, the

Table 1. Change in the explanatory power of the regression model for each variable

	Response variables		
Explanatory variables	**IMC/V**	**SA/V**	**ITC/V**
Tamoxifen	0.07	**<0.01**	0.313
ER	**0.05**	**0.05**	0.82
HER2	0.05	0.05	0.81
Nodes	0.56	0.12	0.65
Tamoxifen.ER	0.22	0.39	0.68
Tamoxifen.HER2	0.67	0.43	0.96
HER2.ER	0.42	0.83	0.46
Tamoxifen.Nodes	0.64	0.83	0.79
ER.Nodes	0.51	**0.02**	0.13

P-values for the F-test on the change in the explanatory power of the regression model for each variable (tamoxifen treatment, ER, HER2 and lymph node status) and combination of variables introduced with respect to models for response variables (IMC/V, SA/V and ITC/V). Significant effects are highlighted in bold.

Table 2. Change in the explanatory power of the regression model for each variable for ER+ and ER– tumours

	Response variables		
Explanatory variables	**IMC/V**	**SA/V**	**ITC/V**
ER+ tumours			
Tamoxifen	0.515	**0.05**	0.727
HER2	0.10	0.33	0.56
Nodes	0.63	0.61	0.38
Tamoxifen.HER2	0.55	0.26	0.87
ER– tumours			
Tamoxifen	**0.05**	**0.03**	0.09
HER2	0.21	**0.05**	0.40
Nodes	0.26	**0.03**	**0.05**
Tamoxifen.HER2	0.77	0.90	0.99

P-values for the F-test on the change in the explanatory power of the regression model for each variable (tamoxifen treatment, HER2 and lymph node status) and combination of variables introduced with respect to models for response variables (IMC/V, SA/V and ITC/V). Results are for ER+ and ER– tumours. Significant effects are highlighted in bold.

IMC/V value was significantly smaller for treated tumours than for untreated tumours [treated IMC/V −7451.83±1406.29; untreated IMC/V −11394.87±4243.42; $t(20)=2.09$, $P=0.02$]. Likewise, SA/V was significantly lower for treated tumours compared with untreated tumours [treated 193.91±15.01; untreated 245.28±42.67; $t(20)=3.26$, $P<0.01$]. There were no other significant differences in morphological characteristics for HER2+ or HER2– tumours.

In addition to biological status, we also quantified changes in proliferative and apoptotic activity in tumour materials, by staining for Ki67 and cleaved caspase-3, respectively, for a subset ($n=6$) of tumours with available data (Leeper et al., 2012). We assessed the correlation between both Ki67 and cleaved caspase-3 levels and the Minkowski functionals in both treated and untreated tumours. In treated tumours, we observed a near-significant and moderately strong negative correlation between Ki67 levels and IMC/V ($R=-0.79$; $P=0.06$ Spearman rank, $n=6$) and the same strong negative correlation for caspase-3 expression (not significant) ($R=0.62$, $P=0.18$ Spearman rank, $n=6$). All other correlations were not significant.

Linking Minkowski functionals to tumour grade

Finally, we investigated the extent to which the Minkowski functionals (normalised by volume) could be used to predict tumour grade. Clinically, tumours are graded by pathologists, independently of expected treatment, ER status or HER2 status. Discriminant factor analysis, a well-known modelling approach for prediction of a dependent categorical value from independent variables (Boehm et al., 2008), was performed to predict tumour grade (1, 2 or 3) using IMC/V, SA/V and ITC/V as independent variables. The resulting classification table (Table 4) indicates that the Minkowski functionals provided excellent predictive power for three out of four categories. Grading was based on the tumours observed in the patient and not the tumours in the collagen environment (which were grown from sub-samples of the patient tumour). Morphological characteristics relate to those sub-samples grown in the collagen environment, and we assume that some of morphological characteristics that attracted the grade classification (1, 2 or 3) in vivo persist in the ex vivo experimental culture system.

Our analysis suggests that the morphology of tumours of grade 1 and 2 was not significantly impacted by tamoxifen treatment, although we recognise the small numbers involved. By contrast, tamoxifen had a significant impact on the morphology of grade 3 tumours. Almost all grade 3 tumours that were untreated are classified as grade 3 morphologically. The near-perfect prediction of in vivo grade from in vitro morphology, in spite of limited data, supports our assumption that morphological characteristics persist across sampling and systems. Moreover, we note that the majority (75%) of clinically defined grade 3 tumours, treated with tamoxifen ex vivo, are classified as grade 1 in the culture system. We propose that this significant change in morphology is a consequence of drug action: specifically, that tumours originally re-classified as grade 3 are classified as grade 1 as a result of tamoxifen treatment.

To further explore the relation between grading and Minkowski functionals, we extended our analyses to consider the individual measures used to determine grade. We used the AMN grading system (Elston and Ellis, 1991) in which tumour grade is assessed in terms of acinar or tubule formation, nuclear pleomorphism and mitotic activity, with each element being scored a value of 1 (similar to normal tissue) to 3 (does not resemble normal tissue). Nuclear evaluation and mitotic count is assessed in the worst areas of the sample whereas acinar or tubule formation is evaluated over the whole tumour.

Results of the discriminant factor analysis are shown in Table 5. In untreated tumours, we observed good agreement between the pathological grade and the grade predicted by Minkowski functionals for mitotic count, nuclear pleomorphism and acinar or tubule formation for all tumour grades observed. In treated tumours, we observed good agreement between the pathological grade and that predicted by the Minkowski functionals for mitotic count and nuclear pleomorphism for all tumour grades observed. However, for treated tumours graded according to acinar or tubule formation, only the Minkowski functionals prediction for grade 1 tumours agreed with the pathologist score. For grade 2 and 3 tumours, the Minkowski functionals predicted a grade score that underestimated the grade of tumour (as grade 1). We propose that this specific mis-categorisation reflects the change in tumour-scale

Table 3. Change in the explanatory power of the regression model for each variable for HER+ and HER– tumours

	Response variables		
Explanatory variables	**IMC/V**	**SA/V**	**ITC/V**
HER2+ tumours			
Tamoxifen	0.69	0.40	0.61
ER	0.90	0.30	0.54
Tamoxifen.ER	0.50	0.48	0.77
HER2– tumours			
Tamoxifen	**0.03**	**<0.01**	0.40
ER	0.40	0.93	0.79
Tamoxifen.ER	0.45	0.64	0.88

P-values for the F-test on the change in the explanatory power of the regression model for each variable (tamoxifen treatment and ER status) and combination of variables introduced with respect to models for response variables (IMC/V, SA/V and ITC/V). Results are for HER+ and HER– tumours. Significant effects are highlighted in bold.

Table 4. Classification table of discriminant factor analysis

	Predicted grade			Accuracy
Pathology grading	**1**	**2**	**3**	**(%)**
Grade 1, all tumours	5	0	0	100
Grade 2, all tumours	0	4	0	100
Grade 3, untreated tumours	1	0	12	92.3
Grade 3, treated tumours	6	0	2	25

For grade 1 and grade 2 tumours, Minkowski functions predict grade with 100% accuracy. For grade 3 untreated and treated tumours, Minkowski functions predict with ~92% and 25% accuracy, respectively. SA/V, IMC/V and ITC/V were normally distributed (Kolmogorov-Smirnoff: P=0.683, P=0.545 and P=0.111, respectively).

morphology as characterised by acinar or tubule formation induced by tamoxifen application post-grading.

DISCUSSION

Carcinomas comprise at least 80% of human solid tumours. As the cancer progresses, the transformed epithelia spread locally into the connective tissue (stroma), ultimately forming local and distal metastases (Valastyan and Weinberg, 2011). The spread of cancer thus occurs in 3D space. This has been modelled in vitro using extracellular matrix-based tissue culture models. In breast research, compliant collagen type I or basement-membrane extract have been used successfully in modelling both normal development and cell transformation (Katz et al., 2005; Katz et al., 2010). Nevertheless, the analysis of 3D cultures is almost exclusively undertaken using only 2D techniques, frequently based on analysis of microscopic sections of formalin-fixed sample sections (Katz et al., 2011; Katz et al., 2012). This has resulted in lack of knowledge regarding the 3D morphological properties both of human cancer as it occurs naturally and in 3D culture-based cancer models. Previous work has partly bridged the gap from 2D to 3D: a metric derived from 2D sections (number of cell clusters) carries with it an implicit measure of structure in 3D (Franzén et al., 2008). Such clusters represent fragmentation of the tumour 2D slice and, because the section is a slice through tissue, this fragmentation might represent a tumour structure that in 3D has invasive protrusions and/or tumour budding.

The transition from normal to malignant epithelial tissue involves many morphological changes, such as cellular depolarisation, loss of cellular junctions and alterations in rates of proliferation and apoptosis (Debnath and Brugge, 2005). 3D cultures introduce environmental cues from the extracellular matrix, enabling more accurate modelling of tumour behaviour (Egeblad et al., 2010). Although 3D cultures have been used for study of some cancers including those of the skin (Amjad et al., 2007), breast (Katz et al., 2012) and ovaries (Muranen et al., 2012), their analysis is still performed in single 2D sections.

Here, we have characterised the morphology of cancer spread in 3D using Minkowski functionals (normalised by volume) in primary breast tumours grown in type I collagen matrix. Breast tumours grown in these 3D cultures were analysed, using factorial analysis by regression, on the basis of four important clinical biomarkers: histological grade, ER status, HER2 status and node status. In addition, we analysed tumours treated with tamoxifen, one of the most common drugs used for patients world-wide. Although volume-based analysis has shown that ER+ tumours respond to tamoxifen in agreement with clinical literature (Dowsett et al., 2005), our more detailed morphometric analysis has led to several other observations.

ER status is not a discriminator of tumour morphology, neither in the absence of treatment nor in response to tamoxifen treatment, once Minkowski functionals are normalised with respect to the volume of detected tumour objects. This suggests that change in volume is the correct measurement for tamoxifen response, regardless of ER status, and our earlier work demonstrates that change in volume is a major response to tamoxifen treatment. Lymph node status is only significant in ER– tumours and therefore of limited application in analysis of tamoxifen response. Because HER2 is not a significant explanatory variable for any of Minkowski functionals, HER2 status is not in itself a discriminator of tumour morphology in the absence of treatment. This observation is supported in extensive literature, which failed to find any morphological features unique to HER2+ tumours (Bertos and Park, 2011).

We make the novel observation that HER2 status is a discriminator of a differential morphological response to tamoxifen. Tamoxifen treatment is a significant factor for morphological response variables IMC/V and SA/V for HER2– tumours but not for HER2+ tumours. This observation is also supported in other studies, which showed that HER2 signalling is a mechanism of drug resistance to endocrine treatment such as tamoxifen (Mullen et al., 2007). Our study suggests that morphometric variables can quantify levels of tamoxifen response in sensitive HER2– tumours, and that these morphometrics will remain unchanged in HER2+ tumours.

Lastly, there was high concordance between the original tumour grade, as determined by clinical pathologists, and that predicted by analysis based on Minkowski functionals. Furthermore, tamoxifen treatment lowered the grade, as expected. Our detailed analysis showed that this is linked to restoration of acinar and tubule formation in treated tumours. This novel observation might link good response to tamoxifen to reformation of normal breast tissue components, such as cell-cell junctions (Lanigan et al., 2009).

The current study utilised primary tumour material grown in 3D ex vivo. These cultures contain large bodies, each containing thousands of cells (Leeper et al., 2012). Nonetheless, analysis based on Minkowski functionals can be readily applied to other 3D studies

Table 5. Classification table of discriminant factor analysis with respect to mitotic count, nuclear pleomorphism and acinar or tubule formation

	Predicted grade			Agreement
Pathology grading	1	2	3	(%)
Mitotic count				
Untreated grade 1	5*	0	0	100
Untreated grade 2	1	7*	0	87.5
Untreated grade 3	1	0	4*	80
Treated grade 1	4*	0	0	100
Treated grade 2	1	3*	0	75
Treated grade 3	0	0	4*	100
Nuclear pleomorphism				
Untreated grade 2	0	5*	0	100
Untreated grade 3	0	2	11*	84.6
Treated grade 2	0	4*	0	100
Treated grade 3	0	2	6*	75
Acinar or tubule formation				
Untreated grade 1	3*	0	0	100
Untreated grade 2	0	3*	0	100
Untreated grade 3	0	0	12*	100
Treated grade 1	2*	0	0	100
Treated grade 2	2	0*	0	0
Treated grade 3	8	0	0*	0

*The number of grade predictions made using the Minkowski functionals that agree with pathology grades based separately on mitotic count, nuclear pleomorphism and acinar or tubule formation.

of epithelial morphology. Previous attempts to define 3D morphology in the context of cancer relied on smaller scale structures, containing hundreds of cells at the most. Furthermore, these classifications are frequently qualitative. For example, Bissell and co-workers categorised all 3D structures formed by breast cancer cells into round, mass, grape-like and stellate formations (Kenny et al., 2007). Subsequent morphological analysis was insufficient to discriminate between round and mass types and ultimately settled on three subtypes (Han et al., 2010). Although this type of analysis is useful for a broad molecular understanding of 3D structures, it is lacking as a quantitative measure to express the enormous variability found in human tumours.

The dynamic description offered by using four Minkowski functionals is a well-developed and powerful analytical approach. It accurately defines morphological variability in human tumours by quantitative geometric and topological analysis. This type of analysis should enable more in-depth association of known biomarkers with epithelial cancer morphology, as well as better explaining the response or insensitivity of particular tumours to treatment. The use of cancer microtissues in high-throughput screening of drug responses offers a particularly relevant application (Drewitz et al., 2011; Sundstrom et al., 2012). Such an approach is usually based on volumetric analysis of 3D spheroids or on area measurements of 2D projections. Our Minkowski functionals-based approach can be directly applied in this context to glean further information regarding drug responses, similarly to the studies on the effects of tamoxifen described here. A remaining challenge is to quantitatively analyse the extent of stroma involvement before and after treatment ex vivo, because this feature of the tumour is far less uniformly organised than the epithelia.

METHODS

Tumours, ex vivo culture and OPT data generation

Our data set is based on 3D cultures of primary breast cancer explants growing ex vivo in the presence of estrogen with or without tamoxifen (Leeper et al., 2012). The culture system is fully described (Leeper et al., 2011). Briefly, multiple core biopsies were harvested from consenting patients at the time of curative surgical resection for invasive breast cancer. Cores were divided by eye using a scalpel into 1 mm^3 explants. Explants were cultured in a type I collagen matrix (0.3 mg/ml) for 20 days in the presence of 1.6×10^{-10} M β-estradiol (estrogen). At day 8 of culture, half of the growing explants continued to receive only estrogen, and the other half received estrogen and 4×10^{-6} M tamoxifen for the remaining 12 days (Leeper et al., 2012). The resulting culture materials were stained with anti-cytokeratin antibody following a standard protocol, and scanned using an optical projection tomograph (OPT; Bioptonics 3001M).

For analysis, we had 420 individual 2D image scans for each tumour. These 2D projections were reconstructed into 3D volume images using NRecon software. In our data set, we had 30 tumours comprising five ER+, HER2+ tumours; 12 ER+, HER2– tumours; three ER–, HER2+ tumours; and ten ER–, HER2– tumours. Five of the tumours were grade 1, four were grade 2 and 21 were grade 3. Of the 30 tumours, 12 were treated with tamoxifen and 18 were untreated. Supplementary material Table S1 provides the ER and HER2 status (±) and tamoxifen treatment (yes or no) for each tumour. Following reconstruction, volume images were exported as slices in the BMP file format; this allowed the volume data to be easily imported into image analysis packages such as FIJI (ImageJ).

The ER, HER2 and lymph node status and tumour grade were determined separately by qualified pathologists for 15 breast cancers as part of the clinical process.

Minkowski functionals

Minkowski functionals are a set of measures that provide a quantitative description of geometric and topological structure in *n*-dimensional space. In 2D Euclidean space, morphology can be quantified by the three measures: area fraction, boundary length and the Euler number (Mattfeldt et al., 2007), where the Euler number describes the connectivity of objects detected within an image (Legland et al., 2007). In 3D Euclidean space, the Minkowski functionals are related (by dimensional scaling factors) to volume, surface area, IMC and ITC, which in turn is related to the Euler characteristic (χ) by a dimensional scale factor (Arns et al., 2010). In most cases (such as the work presented here), analysis is carried out on data having a constant dimensionality (typically either 2D or 3D) and so a dimensional scaling factor is less important; such factors are cancelled by taking ratios between the measures. More generally, the fundamental morphological properties of objects within D dimensional space are characterised by D+1 Minkowski functionals (Schmalzing and Buchert, 1997). Because of the general applicability of the Minkowski functionals to any data set, these metrics have already been used in a wide range of fields. For

example in 3D data sets, Minkowski functionals analysis of magnetic resonance images can effectively predict the mechanical properties of trabecular bone (Boehm et al., 2008). Minkowski functionals analysis has revealed insights into galaxy clustering structures and given confidence in other models of galaxy structure (Hikage et al., 2003). In materials science, Minkowski functionals have been employed to help understand the dynamics of models of the microstructure properties of foams (Lautensack and Sych, 2006). In soil science, Minkowski functionals have been used to characterise soil morphology (Falconer et al., 2012). Likewise, our data sets concern 3D space and, although volume and surface area are self-explanatory, IMC and ITC benefit from additional description here (see also Arns et al., 2010).

In 3D space, any non-spherical curved surface exhibits two principal curvatures at each point on its surface (whereas a spherical surface exhibits constant curvature in all directions at all points on its surface). These principal curvatures are measured orthogonally and can be referred to as the major and minor curvatures. The mean curvature, as the name suggests, is found by taking the arithmetic mean average of these major and minor curvature measures, and so the IMC is a summation of this averaged curvature measure over the entire surface. In short, this provides a summary measure of the overall curvedness of the surface. Positive IMC values indicate overall convexity; negative IMC values indicate overall concavity. ITC is a purely topological measure describing connectedness according to some local neighbourhood of the image elements. In the 3D case (as in the work presented here) the six-connected (Von-Neumann) neighbourhood is used. In the case of digital images, ITC is – in simple terms – estimated as the sum of the number of regions or clusters of connected image elements (2D pixels or 3D voxels) comprising the objects of interest added to the number of completely enclosed background regions minus the number of tunnels, i.e. background regions piercing connected object regions. Consequently, a large ITC value represents a largely disjointed pattern. By combining volume, surface area, IMC and ITC, the fundamental measures of both geometry and topology are represented by Minkowski functionals. We use established estimation algorithms (Ohser and Mücklich, 2000) and implement them (Falconer et al., 2012) to characterise 3D morphology of porous media and the simulated distribution of both water and fungal biomass within the pore space.

Image processing and analysis

For image processing, we used FIJI (http://fiji.sc/), an open source distribution, with a range of additional software libraries, of the ImageJ image processing software suite (ImageJA 1.45b, open source software, National Institutes of Health, Bethesda, MD). FIJI was used to process the 2D slice images obtained from the volume reconstruction of OPT scans. The images were filtered and then segmented to produce clear boundaries of the embedded tumours. Specifically, image stacks were imported into FIJI and the images despeckled and outliers removed using the standard operators provided by FIJI. Subsequently, the widely used Otsu method for thresholding (also available as standard in FIJI) was applied. Following thresholding, images were despeckled once again. These segmented and thresholded 3D tomography images were analysed using the estimators described by Ohser and Mücklich (Ohser and Mücklich, 2000) and implemented by Falconer et al. (Falconer et al., 2012) to obtain estimates for each tumour of the four Minkowski functional measures, i.e. the volume fraction, surface area, IMC and ITC.

Statistical analysis

The factorial analysis of variance by regression was undertaken using Genstat 10.1 statistical analysis software. The *t*-tests together with discriminant functional analysis and normality tests were carried out using Microsoft Excel supplemented with XLStat (www.xlstat.com).

ACKNOWLEDGEMENTS

We thank Sandy Leeper and MRC Technology (Edinburgh) for conducting the original ex vivo cultures and facilitating OPT scanning, and Jeremy Thomas (Western General Hospital, Edinburgh) for valuable breast pathology advice.

COMPETING INTERESTS

The authors declare that they do not have any competing or financial interests.

AUTHOR CONTRIBUTIONS

E.K. and D.J.H. conceived and facilitated the ex vivo culture experiments and the use of OPT scanning. J.B. conceived the original idea of the application of Minkowski functionals to 3D tumour data and advised on the content and focus of the study. A.S. led the analysis of the OPT scan data, generated all Minkowski functionals data, contributed to the writing of the interpretation of Minkowski functionals and to the Introduction, and undertook the discriminant analysis for grading. A.E. carried out the initial exploratory analysis and provided the factorial analysis of variance and validation of results. R.F. provided expertise in image analysis software use and, in particular, image thresholding and segmentation essential to the analysis. A.H. developed the Minkowski functionals and estimation algorithms and provided guidance on their usage and interpretation. All authors participated in writing the paper. The final manuscript was edited by E.K. and J.B.

FUNDING

This work was supported by the Northwood Trust (A.S., A.E., J.B.), the Scottish Alliance for Geoscience, Environment and Society (R.F.) and Scottish Funding Council (D.J.H.). Clinical specimens were originally obtained through the Cancer Research UK-supported Edinburgh Experimental Cancer Medicine Centre.

SUPPLEMENTARY MATERIAL

Supplementary material for this article is available at
http://dmm.biologists.org/lookup/suppl/doi:10.1242/dmm.009886/-/DC1

REFERENCES

Amjad, S. B., Carachi, R. and Edward, M. (2007). Keratinocyte regulation of TGF-beta and connective tissue growth factor expression: a role in suppression of scar tissue formation. *Wound Repair Regen.* **15**, 748-755.

Arns, C. H., Knackstedt, M. A. and Mecke, K. (2010). 3D structural analysis: sensitivity of Minkowski functionals. *J. Microsc.* **240**, 181-196.

Beck, A. H., Sangoi, A. R., Leung, S., Marinelli, R. J., Nielsen, T. O., van de Vijver, M. J., West, R. B., van de Rijn, M. and Koller, D. (2011). Systematic analysis of breast cancer morphology uncovers stromal features associated with survival. *Sci. Transl. Med.* **3**, 108.

Bedin, V., Adam, R. L., de Sá, B. C., Landman, G. and Metze, K. (2010). Fractal dimension of chromatin is an independent prognostic factor for survival in melanoma. *BMC Cancer* **10**, 260.

Bertos, N. R. and Park, M. (2011). Breast cancer–one term, many entities? *J. Clin. Invest.* **121**, 3789-3796.

Boehm, H. F., Schneider, T., Buhmann-Kirchhoff, S. M., Schlossbauer, T., Rjosk-Dendorfer, D., Britsch, S. and Reiser, M. (2008). Automated classification of breast parenchymal density: topologic analysis of x-ray attenuation patterns depicted with digital mammography. *AJR Am. J. Roentgenol.* **191**, W275-W282.

Debnath, J. and Brugge, J. S. (2005). Modelling glandular epithelial cancers in three-dimensional cultures. *Nat. Rev. Cancer* **5**, 675-688.

Dowsett, M., Smith, I. E., Ebbs, S. R., Dixon, J. M., Skene, A., Griffith, C., Boeddinghaus, I., Salter, J., Detre, S., Hills, M. et al. (2005). Short-term changes in Ki-67 during neoadjuvant treatment of primary breast cancer with anastrozole or tamoxifen alone or combined correlate with recurrence-free survival. *Clin. Cancer Res.* **11**, 951s-958s.

Drewitz, M., Helbling, M., Fried, N., Bieri, M., Moritz, W., Lichtenberg, J. and Kelm, J. M. (2011). Towards automated production and drug sensitivity testing using scaffold-free spherical tumor microtissues. *Biotechnol. J.* **6**, 1488-1496.

Egeblad, M., Nakasone, E. S. and Werb, Z. (2010). Tumors as organs: complex tissues that interface with the entire organism. *Dev. Cell* **18**, 884-901.

Elston, C. W. and Ellis, I. O. (1991). Pathological prognostic factors in breast cancer. I. The value of histological grade in breast cancer: experience from a large study with long-term follow-up. *Histopathology* **19**, 403-410.

Eynard, H. G., Soria, E. A., Cuestas, E., Rovasio, R. A. and Eynard, A. R. (2009). Assessment of colorectal cancer prognosis through nuclear morphometry. *J. Surg. Res.* **154**, 345-348.

Falconer, R., Houston, A., Otten, W. and Baveye, P. (2012). Emergent behaviour of fungal dynamics: influence of soil architecture and moisture distribution. *Soil Sci.* **177**, 111-119.

Fanshawe, T. R., Lynch, A. G., Ellis, I. O., Green, A. R. and Hanka, R. (2008). Assessing agreement between multiple raters with missing rating information, applied to breast cancer tumour grading. *PLoS ONE* **3**, e2925.

Franzén, L. E., Hahn-Strömberg, V., Edvardsson, H. and Bodin, L. (2008). Characterization of colon carcinoma growth pattern by computerized morphometry: definition of a complexity index. *Int. J. Mol. Med.* **22**, 465-472.

Goutzanis, L. P., Papadogeorgakis, N., Pavlopoulos, P. M., Petsinis, V., Plochoras, I., Eleftheriadis, E., Pantelidaki, A., Patsouris, E. and Alexandridis, C. (2009). Vascular fractal dimension and total vascular area in the study of oral cancer. *Head Neck* **31**, 298-307.

Han, J., Chang, H., Giricz, O., Lee, G. Y., Baehner, F. L., Gray, J. W., Bissell, M. J., Kenny, P. A. and Parvin, B. (2010). Molecular predictors of 3D morphogenesis by breast cancer cell lines in 3D culture. *PLoS Comput. Biol.* **6**, e1000684.

Hikage, C., Schmalzing, J., Buchert, T., Suto, Y., Kayo, I., Taruya, A., Vogeley, M. S., Hoyle, F., Gott, J. R., III and Brinkmann, J. (2003). Minkowski Functionals of SDSS galaxies I: analysis of excursion sets. *Publ. Astron. Soc. Jap.* **55**, 911-931.

Katz, E., Lareef, M. H., Rassa, J. C., Grande, S. M., King, L. B., Russo, J., Ross, S. R. and Monroe, J. G. (2005). MMTV Env encodes an ITAM responsible for transformation of mammary epithelial cells in three-dimensional culture. *J. Exp. Med.* **201**, 431-439.

Katz, E., Dubois-Marshall, S., Sims, A. H., Faratian, D., Li, J., Smith, E. S., Quinn, J. A., Edward, M., Meehan, R. R., Evans, E. E. et al. (2010). A gene on the HER2 amplicon, C35, is an oncogene in breast cancer whose actions are prevented by inhibition of Syk. *Br. J. Cancer* **103**, 401-410.

Katz, E., Verleyen, W., Blackmore, C. G., Edward, M., Smith, V. A. and Harrison, D. J. (2011). An analytical approach differentiates between individual and collective cancer invasion. *Anal. Cell. Pathol. (Amst.)* **34**, 35-48.

Katz, E., Sims, A. H., Sproul, D., Caldwell, H., Dixon, M. J., Meehan, R. R. and Harrison, D. J. (2012). Targeting of Rac GTPases blocks the spread of intact human breast cancer. *Oncotarget*, **3**, 608-619.

Kenny, P. A., Lee, G. Y., Myers, C. A., Neve, R. M., Semeiks, J. R., Spellman, P. T., Lorenz, K., Lee, E. H., Barcellos-Hoff, M. H., Petersen, O. W. et al. (2007). The morphologies of breast cancer cell lines in three-dimensional assays correlate with their profiles of gene expression. *Mol. Oncol.* **1**, 84-96.

Lanigan, F., McKiernan, E., Brennan, D. J., Hegarty, S., Millikan, R. C., McBryan, J., Jirstrom, K., Landberg, G., Martin, F., Duffy, M. J. et al. (2009). Increased claudin-4 expression is associated with poor prognosis and high tumour grade in breast cancer. *Int. J. Cancer* **124**, 2088-2097.

Lautensack, C. and Sych, T. (2006). 3D image analysis of open foams using random tessellations. *Image Anal. Stereol.* **25**, 87-93.

Leeper, A. D., Farrell, J., Dixon, J. M., Wedden, S. E., Harrison, D. J. and Katz, E. (2011). Long-term culture of human breast cancer specimens and their analysis using optical projection tomography. *J. Vis. Exp.* **53**, 3085.

Leeper, A. D., Farrell, J., Williams, L. J., Thomas, J. S., Dixon, J. M., Wedden, S. E., Harrison, D. J. and Katz, E. (2012). Determining tamoxifen sensitivity using primary breast cancer tissue in collagen-based three-dimensional culture. *Biomaterials* **33**, 907-915.

Legland, D., Kiêu, K. and Devaux, M. (2007). Computation of Minkowski measures of 2D and 3D binary images. *Image Anal. Stereol.* **26**, 83-92.

Mattfeldt, T., Meschenmoser, D., Pantle, U. and Schmidt, V. (2007). Characterization of mammary gland tissue using joint estimators of Minkowski functionals. *Image Anal. Stereol.* **26**, 13-22.

Mullen, P., Cameron, D. A., Hasmann, M., Smyth, J. F. and Langdon, S. P. (2007). Sensitivity to pertuzumab (2C4) in ovarian cancer models: cross-talk with estrogen receptor signaling. *Mol. Cancer Ther.* **6**, 93-100.

Muranen, T., Selfors, L. M., Worster, D. T., Iwanicki, M. P., Song, L., Morales, F. C., Gao, S., Mills, G. B. and Brugge, J. S. (2012). Inhibition of PI3K/mTOR leads to adaptive resistance in matrix-attached cancer cells. *Cancer Cell* **21**, 227-239.

Ohser, J. and Mücklich, F. (2000). *Statistical Analysis of Microstructures in Material Science*. New York, NY: Wiley.

Schmalzing, J. and Buchert, T. (1997). Beyond genus statistics: a unifying approach to the morphology of cosmic structure. *Astrophysical J.* **482**, L1-L4.

Sundstrom, L., Biggs, T., Laskowski, A. and Stoppini, L. (2012). OrganDots–an organotypic 3D tissue culture platform for drug development. *Expert Opin. Drug Discov.* **7**, 525-534.

Valastyan, S. and Weinberg, R. A. (2011). Tumor metastasis: molecular insights and evolving paradigms. *Cell* **147**, 275-292.

Wang, L. M., Kevans, D., Mulcahy, H., O'Sullivan, J., Fennelly, D., Hyland, J., O'Donoghue, D. and Sheahan, K. (2009). Tumor budding is a strong and reproducible prognostic marker in T3N0 colorectal cancer. *Am. J. Surg. Pathol.* **33**, 134-141.

Wöhlke, M., Schiffmann, L. and Prall, F. (2011). Aggressive colorectal carcinoma phenotypes of invasion can be assessed reproducibly and effectively predict poor survival: interobserver study and multivariate survival analysis of a prospectively collected series of 299 patients after potentially curative resections with long-term follow-up. *Histopathology* **59**, 857-866.

Yaffe, M. J. (2008). Mammographic density. Measurement of mammographic density. *Breast Cancer Res.* **10**, 209.

Table S1. Association between tamoxifen treatment status and either ER or HER2 status for all tumour explant preparations used

ID	Tam	HER2	ER	SA	IMC	ITC	V	Grade	A	M	N	Node
1	N	-	-	3.71805	−112.521	1331.94	0.014	3	2	3	3	-
2	N	-	-	2.15997	−109.619	6096.12	0.01	3	2	3	3	-
3	N	-	-	0.814787	−53.9158	149.87	0.003	3	3	2	3	+
4	N	-	-	1.50304	−55.3955	1129.3	0.006	3	3	2	3	+
5	N	-	-	2.61339	−157.79	15070.9	0.014	3	3	3	3	-
6	N	-	-	1.75235	−114.633	9526.25	0.008	3	3	3	3	-
7	N	-	+	0.969115	−81.0478	11214.4	0.005	1	3	2	3	+
8	N	-	+	3.74823	−167.097	5102.44	0.014	1	3	2	3	-
9	N	-	+	4.08243	−142.723	324.015	0.017	3	3	2	3	-
10	N	-	+	2.75507	−79.0427	626.393	0.013	3	1	1	2	-
11	N	-	+	2.49337	−79.2312	−2267.05	0.012	3	1	1	2	-
12	N	-	+	2.78076	−87.8393	−184.171	0.009	3	3	2	3	+
13	N	-	+	3.00992	−111.694	1629.05	0.011	1	3	2	3	+
14	N	-	+	0.997003	−55.0545	2619.56	0.004	3	1	1	2	-
15	N	+	-	1.31535	−76.5772	2160.98	0.005	3	3	2	3	+
16	N	+	+	3.74723	−141.538	−2855.45	0.016	2	3	1	2	-
17	N	+	+	0.441179	−35.582	3248.06	0.002	2	2	3	3	-
18	N	+	+	3.56894	−143.673	2295.02	0.017	3	3	1	2	-
19	Y	-	-	2.5846	−75.4911	2863.36	0.014	3	2	3	3	-
20	Y	-	-	1.96822	−68.5846	1363.61	0.009	3	2	3	3	-
21	Y	-	-	1.60913	−62.6364	4382.64	0.009	3	3	3	3	-
22	Y	-	-	1.97023	−102.94	3107.17	0.011	3	3	3	3	-
23	Y	-	+	1.67211	−77.8919	4412.2	0.008	3	3	2	3	+
24	Y	-	+	2.82405	−95.1963	−1391.58	0.014	1	1	1	2	-
25	Y	-	+	0.558794	−21.2854	1435.38	0.003	1	1	1	2	-

ID	Tam	HER2	ER	SA	IMC	ITC	V	Grade	A	M	N	Node
26	Y	-	+	3.39935	–118.119	2200.03	0.018	3	3	2	3	-
27	Y	+	-	2.28628	–94.6485	299.74	0.009	3	3	2	3	+
28	Y	+	-	2.64124	–124.631	–795.789	0.011	3	3	2	3	+
29	Y	+	+	1.55899	–99.5469	4087.65	0.006	2	3	1	2	-
30	Y	+	+	0.917186	–51.573	2109.26	0.004	2	3	1	2	-

For each of the 30 tumours, the table shows ER, HER2, lymph node status and whether the tumour has been treated with tamoxifen (Y) or not (N). Additionally, Minkowski functionals used in the analysis (SA, IMC, ITC and V) are provided as absolute values. Tumour grading information (overall grade, A, M and N) and node status are included.